Vibro-acoustic analysis of lightweight composite panels with damping materials

L.C. Cardoso[1,2], J. Dias Rodrigues[1]

[1]Faculdade de Engenharia da Universidade do Porto (FEUP), Departamento de Mecânica,
R. Dr. Roberto Frias, 4200-465 Porto, Portugal
[2]Instituto de Engenharia Mecânica e Gestão Industrial (INEGI), Universidade do Porto, Campus da FEUP,
R. Dr. Roberto Frias, 400, 4200-465 Porto, Portugal
email: lc.cardoso@fe.up.pt, jdr@fe.up.pt

ABSTRACT: In this paper a numerical model to study the vibro-acoustic behavior of a laminated plate backed by a poroelastic foam layer is developed. Such approach consists on a coupled mitigation strategy aiming either mechanical vibration suppression or acoustic attenuation as well. The laminated plate model consists of fiber laminae with interleaved viscoelastic layers in standard constrained or integrated layer damping schemes, whereas surface mounted poroelastic foam materials are included. Mechanical and acoustic excitations in terms of incident plane waves are considered in this study. For the plate modeling, the finite element method considering a layerwise kinematic assumption is used. On the other hand, poroelastic treatments are developed based on the Biot's theory of poroelasticity. As a result, using the capabilities of the multi-layered model, different vibro-acoustic indicators characterizing the vibro-acoustic behavior of panels vibrating in an acoustic fluid are computed, namely, mean square velocity, radiation sound power, radiation efficiency and transmission loss of the coupled fluid-plate system. In addition, a study addressing the coupling between both solid and fluid phases of the poroelastic material in the plate-foam coupled design is performed aiming to study about the energy dissipation and sound mitigation performance of the poroelastic treatment.

KEY WORDS: Vibro-acoustics; Biot's theory; Poroelastic; Viscoelastic; Damping; Composite.

1 INTRODUCTION

Lightweight composite panels used in automotive and aerospace constructions suffer from low acoustic performance when subjected to mechanical and/or acoustic excitations. Many research efforts have been done towards to develop passive damping technologies to control vibrations and acoustic problems by exploring damping properties of polymer-based materials embedded onto laminated components. Therewith, for an accurately prediction of the behavior of laminated components several finite element models have been developed. In general, the equivalent single layer model or the layerwise model are employed. In the equivalent single layer model the multi-layer structure is considered as a unique homogeneous layer for which equivalent mechanical properties are derived. On the other hand, a layerwise model takes each layer separately which allows for an effective modeling of the deformation process in multi-material laminated structures [1].

Regarding the vibration control through passive damping technologies, those using viscoelastic materials interleaved with stiff isotropic elastic layers have been extensively applied to suppress resonant mechanical behavior [2–4] and sound radiation problems [5–8]. The open literature regarding vibrations and sound radiation from fiber composite structures is less abundant. However, the anisotropic characteristics of the laminae allows for a well-suited design in terms of damping treatments [9, 10] with respect to vibro-acoustic performance. In the present work the constrained damping treatment consisting of a thin viscoelastic layer embedded into the main vibrating component and covered with a stiffer elastic layer is studied, which constitutes, in general, the most effective damping configuration owing to higher amount of energy dissipated caused by high transverse shear deformations developed within viscoelastic layer due to the translation of the neutral plane caused by the constraining layer.

In conjunction with viscoelastic materials further control solutions by using porous materials are increasingly applied for noise control purposes owing to their sound absorption features due to its porous and filamentous microstructure being frequently used in a structure-lined design, bonded, unbounded or mounted closed to the main vibrating component. A certain class of porous foams with flexible skeleton exhibits viscoelastic behavior contributing either for airborne noise mitigation or further structural damping [11]. The porous materials considered in this work are those consisting of an elastic frame (solid phase) saturated by an acoustic fluid (fluid phase). The behavior of such materials can effectively be predicted by using the Biot's theory of poroelasticity [12, 13] for which various formulations were developed in the last decade and half. In the present work, the mixed-displacement pressure formulation [14] is used, which is an exact formulation with respect to the Biot model.

The sound radiation from non-porous structures has been investigated along the past decades. However, the literature focusing the radiation behavior of porous foams is still scarce. In a recent paper, Atalla et al. [15] presented an extended integral weak formulation for Biot's equations considering further virtual work contributions of the radiated pressure using Rayleigh integral. The authors show that the proposed radiation impedance approach allows for an improved accounting of the

radiation damping near to resonance frequencies. In addition, they also concluded that porous foams have small radiation efficiency what constitutes a motivation to use such foams as free-layer sound absorbing treatments mounted in efficient radiators. The porous materials are often acoustically characterized considering airborne excitations with porous sample mounted over a rigid surface. Under these conditions, porous performance indicators may only be valid for acoustic excitations, disregarding the radiation behavior arising from low-frequency mechanical excitations provided from vibrations of host components. A few research has been conducted to consider the influence of the base motion on absorption performance of porous materials [16–18]. In the present study, this issue is studied considering orthotropic components as the base which constitute an enlargement of the state-of-the-art in this field.

This paper presents a numerical approach based on a coupled Finite Element - Rayleigh Integral strategy to study vibroacoustic response from fiber composite panels embedding viscoelastic layers and lined with a sound absorbing poroelastic foam. The present approach is used to predict the dynamics of such a panel immersed in an acoustic domain in which both mechanical and acoustic excitations are applied to the panel. To the author's knowledge, studies devoted on the sound radiation from viscoelastically damped fiber composite structures lined with poroelastic foams was not properly explored regarding the sound radiation process from the porous foam mounted over a vibrating orthotropic panel.

2 THEORETICAL FORMULATION

2.1 Description of mathematical model

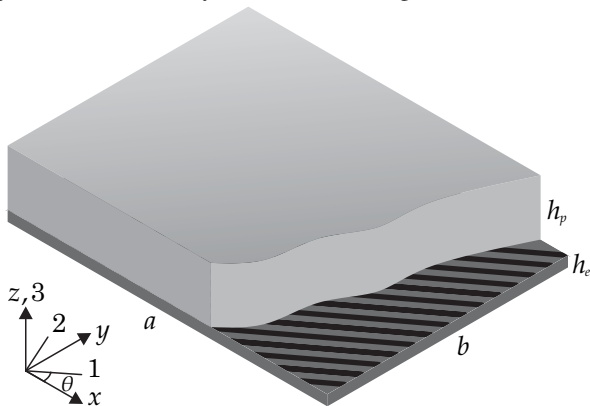The problem under analysis is shown in Fig. 1.

Figure 1. Geometry of the composite plate structure covered by a poroelastic foam. Global reference (x, y, z) and material reference $(1, 2, 3)$.

A rectangular plate is comprised of an elastic plate $(a \times b \times h_e)$ covered by a poroelastic foam $(a \times b \times h_p)$. The elastic plate may be simply isotropic or an anisotropic structure with a generic stacking of isotropic/orthotropic layers. In addition, a viscoelastic layer may be considered embedded to the elastic structure. The entire coupled elasto-visco-porous structure is assumed to be in the reference plane (x, y) located at the middle surface of the elastic plate and placed between two infinite rigid

baffles. One of the baffle separates a semi-infinite acoustic domain for $z < 0$ and the other one for $z > h_p$. Therefore, the entire structure can interact with surrounding acoustic medium on its lower and upper surfaces. The plate may be subjected to harmonic forces provided from mechanical loads and/or acoustic sources.

2.1.1 Composite plate modelling

The displacement field in each layer k of the elastic plate is written as [1],

$$u_k = u_0 + \frac{h_1}{2}\beta_1^x + \sum_{j=2}^{k-1} h_j\beta_j^x + \frac{h_k}{2}\beta_k^x + z_k\beta_k^x$$

$$v_k = v_0 + \frac{h_1}{2}\beta_1^y + \sum_{j=2}^{k-1} h_j\beta_j^y + \frac{h_k}{2}\beta_k^y + z_k\beta_k^y \qquad (1)$$

$$w_k = w_0$$

where u_0, v_0 are the in-plane displacements in the x and y directions and w_0 is the out-of-plane displacement in the transverse direction z of the first layer of the generalized multilayered model. β_k^x and β_k^y are the rotations in the xz and yz planes around the y and x axes, respectively. For each layer the kinematics based on the first-order shear deformation theory (FSDT) is assumed. According to (1) the continuity of interlayer displacements is assured. The model is used here to modelling multilayered composite panels including fiber composite laminates, viscoelastic materials and isotropic laminae.

The governing equations of motion of the plate vibration can be derived using the Hamilton's principle,

$$\delta \int_{t_1}^{t_2} (V - U + W)\mathrm{d}t = 0, \qquad (2)$$

where V, U and W are the kinetic energy, the potential (strain) energy and the work done by the external applied loads, respectively. The kinetic and potential energies of a laminated with N layers are given by the summation of the contributions of each layer k,

$$V = \sum_{k=1}^{N} \frac{1}{2} \int_A \dot{\mathbf{u}}^{\mathrm{T}} \mathbf{J}_k \dot{\mathbf{u}}\mathrm{d}A, \quad U = \sum_{k=1}^{N} \frac{1}{2} \int_A \mathbf{u}^{\mathrm{T}} \mathbf{B}_k^{\mathrm{T}} \mathbf{D}_k \mathbf{B}_k \mathbf{u}\mathrm{d}A, \quad (3)$$

where $\mathbf{u}$ and $\dot{\mathbf{u}}$ are, respectively, the displacement and the velocity vectors, $\mathbf{B}_k$ is the deformation matrix and $\mathbf{J}_k$ is the inertia matrix. The constitutive matrix $\mathbf{D}_k$ for each lamina is given by,

$$\mathbf{D}_k = \begin{bmatrix} h_k\mathbf{C}_k & \mathbf{0} & \mathbf{0} \\ \mathbf{0} & \frac{h_k^3}{12}\mathbf{C}_k & \mathbf{0} \\ \mathbf{0} & \mathbf{0} & h_k\mathbf{G}_k \end{bmatrix}, \qquad (4)$$

where h_k is the layer thickness and $\mathbf{C}_k$ and $\mathbf{G}_k$ are the constitutive matrices in the global reference given by,

$$\mathbf{C}_k = \mathbf{T}_\mathrm{f}\mathbf{C}\mathbf{T}_\mathrm{f}^{\mathrm{T}}, \quad \mathbf{G}_k = \mathbf{T}_\mathrm{s}\mathbf{S}\mathbf{T}_\mathrm{s}^{\mathrm{T}}, \qquad (5)$$

where $\mathbf{T}_\mathrm{f}$ and $\mathbf{T}_\mathrm{s}$ are the transformation matrix from local to global reference for bending and shear elasticity matrices,

$$\mathbf{T}_\mathrm{f} = \begin{bmatrix} c^2 & s^2 & -2cs \\ s^2 & c^2 & 2cs \\ cs & -cs & c^2 - s^2 \end{bmatrix}, \quad \mathbf{T}_\mathrm{s} = \begin{bmatrix} c & -s \\ s & c \end{bmatrix}, \qquad (6)$$

where $c = \cos(\theta)$, $s = \sin(\theta)$ and θ is the angle between the material axis 1 and the global direction x. For an orthotropic lamina the constitutive matrices in the material reference one writes,

$$\mathbf{C} = \begin{bmatrix} C_{11} & C_{12} & 0 \\ C_{12} & C_{22} & 0 \\ 0 & 0 & C_{44} \end{bmatrix}, \quad \mathbf{S} = \begin{bmatrix} C_{55} & 0 \\ 0 & C_{66} \end{bmatrix}, \quad (7)$$

in which the elasticity coefficients are given by,

$$C_{11} = \frac{E_1}{1 - \nu_{12}\nu_{21}}, \quad C_{44} = G_{12}, \quad (8)$$

$$C_{12} = \frac{\nu_{21}E_1}{1 - \nu_{12}\nu_{21}}, \quad C_{55} = G_{13}, \quad (9)$$

$$C_{22} = \frac{E_2}{1 - \nu_{12}\nu_{21}}, \quad C_{66} = G_{23}. \quad (10)$$

For an isotropic layer, the constitutive matrix is defined as,

$$\mathbf{C}_k = \frac{E_k}{1 - \nu_k^2} \begin{bmatrix} 1 & \nu_k & 0 \\ \nu_k & 1 & 0 \\ 0 & 0 & \frac{1-\nu_k}{2} \end{bmatrix}, \quad \mathbf{G}_k = \frac{E_k}{2(1 + \nu_k)} \begin{bmatrix} 1 & 0 \\ 0 & 1 \end{bmatrix}, \quad (11)$$

where E_k and ν_k are the Young's modulus and Poisson's ratio of the material. The virtual work done by an external distributed loading applied to the plate surface one writes,

$$\delta W = \int_S \delta \mathbf{u}^T \mathbf{q} \, dS, \quad (12)$$

where $\mathbf{q}$ is the distributed load and S is the plate area. Applying the Hamilton's principle and assuming a steady harmonic time-dependence $e^{j\omega t}$ the weak form of the composite plate problem can be expressed as follows,

$$\sum_{k=1}^{N} \left(\int_A \delta \mathbf{u}^T \mathbf{B}_k^T \mathbf{D}_k \mathbf{B}_k \mathbf{u} \, dA - \omega^2 \int_A \delta \mathbf{u}^T \mathbf{J}_k \mathbf{u} \, dA \right)$$
$$= \int_S \delta \mathbf{u}^T \mathbf{q} \, dS. \quad \forall (\delta \mathbf{u}) \quad (13)$$

2.1.2 Poroelastic material modeling

The fundamental equations of the Biot's theory of the poroelasticity [12, 13] in conjunction with the frequency-domain mixed displacement-pressure formulation (u, p) [14] are considered here to modeling an isotropic poroelastic foam saturated by an acoustic fluid. The Biot model applied to the poroelastic foam comprises two homogeneous and continuum mediums (a solid phase and fluid phase) which are coupled by inertial and viscous forces developed into the porous medium owing to the relative motion of the solid and fluid particles. In the case of the mixed formulation the primary variables are the fluid pressure p and the solid phase displacements $\mathbf{u}_s = [u_x, u_y, u_z]^T$; the poroelastic model thus requires only four degrees of freedom instead of six ones of the displacement-displacement formulation primarily derived.

Considering the Biot equations and using the principle of the virtual work, the weak form for the poroelastic material yields in the form,

$$\int_{\Omega_p} \varepsilon(\delta \mathbf{u}_s)^T \tilde{\mathbf{D}} \varepsilon \, d\Omega_p - \omega^2 \tilde{\rho} \int_{\Omega_p} \delta \mathbf{u}_s^T \mathbf{u}_s \, d\Omega_p$$
$$+ \frac{\phi^2}{\omega^2 \tilde{\rho}_{22}} \int_{\Omega_p} \nabla \delta p^T \cdot \nabla p \, d\Omega_p - \frac{\phi^2}{\tilde{R}} \int_{\Omega_p} \delta p \cdot p \, d\Omega_p$$
$$- \tilde{\gamma} \int_{\Omega_p} \nabla \delta p^T \cdot \mathbf{u}_s \, d\Omega_p$$
$$- \tilde{\gamma} \int_{\Omega_p} \delta \mathbf{u}_s^T \cdot \nabla p \, d\Omega_p - \int_{\partial \Omega_p} \phi(\mathbf{u}_f - \mathbf{u}_s) \mathbf{n} \delta p \, d\Gamma$$
$$- \int_{\partial \Omega_p} \delta \mathbf{u}_s^T \hat{\sigma}_p \mathbf{n} \, d\Gamma = 0, \quad \forall (\delta \mathbf{u}_s, \delta p) \quad (14)$$

where $\hat{\sigma}_p$ and ε are, respectively, the total stress tensor and the strain tensor of the solid phase, $\tilde{\mathbf{D}}$ is the elasticity matrix of the solid phase which may accounts for damping in the solid skeleton, $\mathbf{u}_s$ and $\mathbf{u}_f$ are the macroscopic displacements of the solid and fluid phases, respectively, $\tilde{R}$ is the bulk modulus of the air within a fraction ϕ of the volume of the porous material and $\tilde{\rho}$ and $\tilde{\rho}_{22}$ are the effective densities of the solid phase and the fluid phase, respectively. $\mathbf{n}$ is the unit normal vector outwards from the boundary, $\hat{\sigma}_p \cdot \mathbf{n}$ stands for external surface forces per unit area along the normal direction at the boundary surface $\partial \Omega_p$. The parameter $\tilde{\gamma}$ is defined as follows,

$$\tilde{\gamma} = \phi \left(\frac{\tilde{\rho}_{12}}{\tilde{\rho}_{22}} - \frac{\tilde{Q}}{\tilde{R}} \right), \quad (15)$$

where $\tilde{Q}$ is the elastic coupling coefficient between the solid and fluid phases. Ω_p and $\partial \Omega_p$ denote, respectively, the poroelastic domain and its boundary and ω is the angular frequency.

2.1.3 Continuity coupling plate-foam

The poroelastic foam is considered perfectly bonded to the composite plate. Therefore, appropriate interface conditions have to be satisfied at the plate-foam interface to ensure continuity of normal stresses, the zero relative mass flux between the porous solid and fluid phases across the interface and the displacement continuity between both solid domains. Those interface restraints can be conveniently written in the form,

$$\hat{\sigma}_p \mathbf{n} = \sigma_e \mathbf{n}, \quad (16)$$

$$\phi(\mathbf{u}_f - \mathbf{u}_s) \mathbf{n} = 0, \quad (17)$$

$$\hat{\mathbf{u}}_p = \mathbf{u}_e, \quad (18)$$

where σ_e is the elastic (plate) stress tensor, $\hat{\mathbf{u}}_p$ and $\hat{\sigma}_p$ are the total displacement vector and stress tensor of the porous material, respectively, and $\mathbf{u}_e$, $\mathbf{u}_f$ and $\mathbf{u}_s$ are the displacement vectors of the elastic (plate), porous fluid phase and solid phase, respectively. $\mathbf{n}$ is the interface normal vector and ϕ is the porosity. Once the coupling between the poroelastic domain and the elastic domain is natural [19] only the kinematic condition (18) has to be explicitly imposed on the plate-foam interface. To this end, in this work the *Lagrange multipliers method* is used to enforce the normal continuity of both elastic plate and solid phase displacement fields.

2.1.4 Viscoelastic damping modelling

The viscoelastic material considered throughout this work is the ISD-112 of 3M in which the frequency-dependent mechanical properties are determined using the three-series *Anelastic Displacement Field* model for a temperature of 27°C. In terms of the finite element implementation the complex modulus approach is considered for which the mechanical properties of the viscoelastic material are given in terms of the complex shear modulus,

$$G(\omega) = G'(\omega)[1 + j\eta(\omega)], \qquad (19)$$

in which $G(\omega)$ stands for the frequency-dependent shear modulus and $\eta(\omega)$ is the loss factor of the material,

$$\eta(\omega) = \frac{G''(\omega)}{G'(\omega)}, \qquad (20)$$

where $G'(\omega)$ and $G''(\omega)$ are, respectively, the shear storage modulus and the shear loss modulus, the latter accounting for energy dissipation effect. In addition, once the Poisson's ratio can be reasonably taken as frequency-independent the extensional modulus can be easily taken on the model implementation. Fig. (2) shows the frequency dependency of the viscoelastic properties in terms of the shear storage modulus and the loss factor of the material ISD-112 over the frequency range $[0 - 1000]$ Hz.
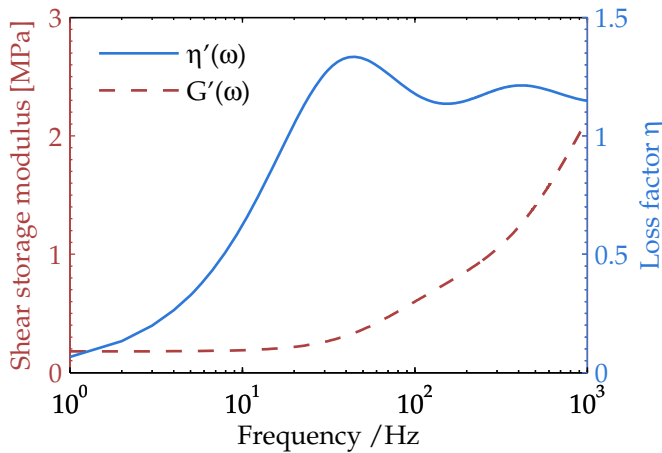

Figure 2. Frequency dependency of the viscoelastic properties of the material 3M ISD-112 at 27°C, used in this study. Shear storage modulus $G'(\omega)$ and loss factor $\eta(\omega)$.

2.2 Finite element implementation

The variational forms of the elastic plate and poroelastic foam domains, given respectively in Eqs. (13) and (14), are discretized using the Galerkin finite element method. In that sense, for poroelastic problem the following mapping is considered,

$$\mathbf{u}_s = \mathbf{N}_s \mathbf{U}_s, \quad \mathbf{p} = \mathbf{N}_f \mathbf{P}, \qquad (21)$$

where $\mathbf{U}_s$ and $\mathbf{P}$ are the vectors of nodal displacements of the solid phase and nodal pressures, respectively, $\mathbf{N}$ are the interpolation functions within the finite element and the subscripts

s and f denote the solid and the fluid component, respectively. The discretization of the variational form given in (14) yields,

$$\int_{\Omega_p} \varepsilon(\delta \mathbf{u}_s)^{\mathrm{T}} \tilde{\mathbf{D}} \varepsilon \, d\Omega_p \Longrightarrow \delta \mathbf{U}^{\mathrm{T}} \mathbf{K}_s \mathbf{U}, \qquad (22)$$

$$\int_{\Omega_p} \delta \mathbf{u}_s^{\mathrm{T}} \mathbf{u}_s \, d\Omega_p \Longrightarrow \delta \mathbf{U}^{\mathrm{T}} \mathbf{M}_s \mathbf{U}, \qquad (23)$$

$$\int_{\Omega_p} \delta \mathbf{u}_s^{\mathrm{T}} \cdot \nabla p \, d\Omega_p \Longrightarrow \delta \mathbf{U}^{\mathrm{T}} \mathbf{H}_{sf} \mathbf{P}, \qquad (24)$$

$$\int_{\Omega_p} \nabla \delta p^{\mathrm{T}} \cdot \nabla \delta p \, d\Omega_p \Longrightarrow \delta \mathbf{P}^{\mathrm{T}} \mathbf{K}_f \mathbf{P}, \qquad (25)$$

$$\int_{\Omega_p} \delta p \cdot p \, d\Omega_p \Longrightarrow \delta \mathbf{P}^{\mathrm{T}} \mathbf{M}_f \mathbf{P}, \qquad (26)$$

$$\int_{\Omega_p} \nabla \delta p^{\mathrm{T}} \cdot \mathbf{u}_s \, d\Omega_p \Longrightarrow \delta \mathbf{P}^{\mathrm{T}} \mathbf{H}_{fs} \mathbf{U}, \qquad (27)$$

In addition, $\delta \mathbf{U}_s$ and $\delta \mathbf{P}$ as well can be arbitrary (stationarity condition) leading to the following system of discrete equations,

$$\begin{bmatrix} \mathbf{K}_s - \omega^2 \mathbf{M}_s & \mathbf{H}_{sf} \\ \mathbf{H}_{fs} & \mathbf{K}_f/\omega^2 - \mathbf{M}_f \end{bmatrix} \begin{Bmatrix} \mathbf{U}_s \\ \mathbf{P} \end{Bmatrix} = \begin{Bmatrix} \mathbf{F}_s \\ \mathbf{F}_f/\omega^2 \end{Bmatrix}, \qquad (28)$$

where $\mathbf{M}_s$ and $\mathbf{K}_s$ are the equivalent mass and stiffness matrices for the solid phase, respectively, and $\mathbf{M}_f$, $\mathbf{K}_f$ are the equivalent kinetic and compression matrices for the fluid phase, respectively. $\mathbf{H}_{sf}$ is the volume coupling matrix between both solid phase displacement and fluid pressure and $\mathbf{H}_{fs} = -\mathbf{H}_{sf}^{\mathrm{T}}$. $\mathbf{F}_s$ and $\mathbf{F}_f$ are the load vectors of the applied forces on the solid phase and fluid phase, respectively.

Using similar procedure as for poroelastic problem, the finite element discretization of the variational form for elastic plate given in (13) yields in the form,

$$\sum_{k=1}^{N} \int_A \delta \mathbf{u}^{\mathrm{T}} \mathbf{J}_k \mathbf{u} \, dA \Longrightarrow \delta \mathbf{U}_e^{\mathrm{T}} \mathbf{M}_e \mathbf{U}_e, \qquad (29)$$

$$\sum_{k=1}^{N} \int_A \delta \mathbf{u}^{\mathrm{T}} \mathbf{B}_k^{\mathrm{T}} \mathbf{D}_k \mathbf{B}_k \mathbf{u} \, dA \Longrightarrow \delta \mathbf{U}_e^{\mathrm{T}} \mathbf{K}_e \mathbf{U}_e. \qquad (30)$$

The stationarity condition leads to the following system of discrete equations for elastic composite plate,

$$\left[\mathbf{K}_e(\omega) - \omega^2 \mathbf{M}_e \right] \mathbf{U}_e = \mathbf{F}_e, \qquad (31)$$

where $\mathbf{M}_e$ is the consistent mass matrix of the composite panel and $\mathbf{K}_e(\omega) = \mathbf{K}_{el} + \mathbf{K}_v(\omega)$ where $\mathbf{K}_{el}$ is the stiffness matrix of the composite elastic plate and $\mathbf{K}_v(\omega)$ is the frequency-dependent stiffness matrix of the viscoelastic layer defined according the complex modulus approach. $\mathbf{F}_e$ is the load vector applied to the elastic plate. The fully coupled plate-foam finite element model yields in the following frequency-domain system

of discrete equations,

$$
\left(
\begin{bmatrix}
\mathbf{K}_e & \mathbf{0} & \mathbf{0} & \mathbf{L} \\
\mathbf{0} & \mathbf{K}_s & \mathbf{0} & \mathbf{R} \\
\mathbf{0} & \mathbf{0} & \mathbf{K}_f & \mathbf{0} \\
\mathbf{L}^{\mathrm{T}} & \mathbf{R}^{\mathrm{T}} & \mathbf{0} & \mathbf{0}
\end{bmatrix}
-\omega^2
\begin{bmatrix}
\mathbf{M}_e & \mathbf{0} & \mathbf{0} & \mathbf{L} \\
\mathbf{0} & \mathbf{M}_s & \mathbf{0} & \mathbf{R} \\
\mathbf{0} & \mathbf{0} & \mathbf{M}_f & \mathbf{0} \\
\mathbf{L}^{\mathrm{T}} & \mathbf{R}^{\mathrm{T}} & \mathbf{0} & \mathbf{0}
\end{bmatrix}
\right)
\begin{Bmatrix}
\mathbf{u}_e \\
\mathbf{u}_s \\
\mathbf{p} \\
\lambda
\end{Bmatrix}
=
\begin{Bmatrix}
\mathbf{F}_e \\
\mathbf{F}_s \\
\mathbf{F}_p \\
\mathbf{0}
\end{Bmatrix}, \quad (32)
$$

where $\mathbf{L}$ and $\mathbf{R}$ accounting for additional constraints involving the free normal degrees of freedom in both plate and foam models.

2.3 Acoustic model

The radiation process considered herein comprises two parts, namely, the radiation describing the transmission from the plate to the acoustic medium and the fluid loading takes into account for the effect of the fluid on the structure. This problem may be accounted by several approaches according to the fluid/structure impedance ratio. For a light fluid, the fluid mass may be neglected and both acoustic and structural problems can be solved independently. For heavy fluids, the problem is more complex owing to strong acoustic radiation damping and added mass effects which may significantly change the inertia of the coupled structure. In the present work we are concerned mainly with radiation involving light fluids such as the air. However, the fluid loading is also considered in the present approach. Considering the plate immersed in an acoustic environment as described previously, each surface pertains to a plane which is rather contained in an infinite plane rigid baffle. In this context, the acoustic radiation from the entire plate may be accounted through the boundary Rayleigh integral approach [20]. Let $p_1(x,y,z)$ and $p_2(x,y,z)$ be the acoustic pressure field in the half-space Ω_1 ($z < 0$) and Ω_2 ($z > h_p$), respectively. Following the Rayleigh integral procedure and considering the Cartesian reference the pressure fields in each half-space are given by the following integral equations,

$$
p_1(\mathbf{r}) = \rho_1 \omega^2 \int_{S^e} G(\mathbf{r},\mathbf{r}_0)w(\mathbf{r}_0)\mathrm{d}S^e, \quad z < 0 \tag{33}
$$

$$
p_2(\mathbf{x}) = -\rho_2 \omega^2 \int_{S^p} G(\mathbf{x},\mathbf{x}_0)w(\mathbf{x}_0)\mathrm{d}S^p, \quad z > h_p \tag{34}
$$

where ρ_1 and ρ_2 are the fluid densities, $G = \mathrm{e}^{-\mathrm{j}kR}/2\pi R$ is the free-field Green's function which satisfies the condition $\partial G/\partial n$ on the rigid baffle, $k = \omega/c$ is the acoustic wave number and R corresponds to the distance between the surface source points $(\mathbf{r}_0, \mathbf{x}_0)$ (integration points) and the receiver points $(\mathbf{r}, \mathbf{x})$ (evaluation points) on the acoustic field. The main advantage of the Finite Element - Rayleigh Integral approach presented in this work is that no additional unknowns are required beyond the structural ones arising from the finite element method. In addition, the weak and strong coupling can suitably be accounted by an acoustic impedance matrix. The main drawback yields from the frequency-dependency of the impedance matrix which usually leads to time-consuming computations. However, in some cases interpolation procedures can be chosen to improve time computations without compromising the accuracy of calculations. The vector of applied forces to the plate accounting for mechanical and fluid forces is given in left-hand side of Eq. (31). The counterpart due to the acoustic load may be written as,

$$
\mathbf{F}_a = \int_S \mathbf{N}^{\mathrm{T}} p\,\mathrm{d}S. \tag{35}
$$

Substituting Eq. (33) into Eq. (35) yields,

$$
\mathbf{F}_a = \omega^2 \rho_1 \mathbf{Z} \mathbf{U}_e, \tag{36}
$$

where $\mathbf{Z}(\omega)$ is the geometrical and frequency-dependent radiation impedance matrix written as,

$$
\mathbf{Z} = \int_S \int_S \mathbf{N}^{\mathrm{T}} G(\mathbf{r},\mathbf{r}_0)\mathbf{N}\,\mathrm{d}S\mathrm{d}S. \tag{37}
$$

The real part of $\mathbf{Z}$ corresponds to the acoustic radiation damping whereas its imaginary part is a measure of the fluid added mass. The numerical evaluation of the radiation matrix is time consuming particularly for higher frequencies where high integration orders are required to get accurate results. A comprehensive review on the evaluation of the radiation impedance matrix calculation is done in [21]. In the present work, the radiation matrix is calculated for the finite element used considering two different numerical integration schemes based on the standard Gauss-Legendre quadrature. The cross-influence coefficients involving non-coincident finite elements are calculated using standard numerical integration where each surface integral contributes in a similar fashion to each matrix coefficient. On the other hand, the self-influence coefficients involving coincident elements require an accurate procedure to deal with the weak singularity appearing in the integrand coming from Green's function. In the present work, a technique based on the Lachat-Watson transformation is used.

The most disadvantage dealing with the radiation matrix $\mathbf{Z}$ lies on its frequency-dependency leading to prohibitive computational times for frequency response calculations. To avoid the calculation of the matrix at each frequency point for a given frequency band of interest, some techniques considering interpolation procedures are available in the literature. However, due to the smoothness of the kernel Green's function with respect to the frequency a simple interpolation can be chosen [5]. In this work, a simple quadratic interpolation is considered. The matrix is calculated at the frequency points ω_i, ω_j and ω_{ij} (with $\omega_i < \omega_{ij} < \omega_j$) and the matrix values between those frequency points are simply interpolated with the following relation,

$$
\mathbf{Z}(\omega) = q_i(\omega)\mathbf{Z}(\omega_i) + q_{ij}(\omega)\mathbf{Z}(\omega_{ij}) + q_j(\omega)\mathbf{Z}(\omega_j), \tag{38}
$$

where the frequency coefficients $q(\omega)$ are the well-known *Lagrange basis functions* written as,

$$
q_i(\omega) = \frac{(\omega - \omega_{ij})(\omega - \omega_j)}{(\omega_i - \omega_{ij})(\omega_i - \omega_j)}, \tag{39}
$$

$$
q_{ij}(\omega) = \frac{(\omega - \omega_i)(\omega - \omega_j)}{(\omega_{ij} - \omega_i)(\omega_{ij} - \omega_j)}, \tag{40}
$$

$$
q_j(\omega) = \frac{(\omega - \omega_i)(\omega - \omega_{ij})}{(\omega_j - \omega_i)(\omega_j - \omega_{ij})}. \tag{41}
$$

2.4 Plate loading

In the present model both acoustic and mechanical loads may be applied on to plate surface. In terms of mechanical loads only point force excitations are of interest here. On the other hand, regarding the acoustic external loads only incident pressure fields by plane waves are considered. For the plate under acoustic loading the total pressure p_t developed on the plate surface is given by,

$$p_t = p_{r1} - p_{r2} + p_b, \tag{42}$$

where p_{r1} and p_{r2} are the radiated pressure fields on the loaded side and free side, respectively, and p_b is the fluid pressure that occurs on the incident side if the plate is perfectly rigid. Considering the plate fully immersed in a light fluid, the pressure caused by the radiation impedances of the fluid medium can reasonably be neglected to the plate loading. Moreover, the pressure radiated on the loaded side may also be disregarded when compared with the blocked pressure p_b. Thus, the pressure load may be given by the blocked pressure which may be approximated by twice the incident pressure [22],

$$p_i(x,y,\omega) = 2\bar{p}_i e^{-j(k_x\xi + k_y\eta)}, \tag{43}$$

where p_i is the frequency-domain incident pressure field generated by an incident plane wave, $\bar{p}_i$ is the amplitude of the incident pressure field and $\xi = x - a/2$ and $\eta = y - b/2$, according to the global reference considered in Fig. (1). The components of the wave vector $\mathbf{k} = \{k_x k_y\}$ in the incident acoustic medium are given by,

$$k_x = k\sin(\theta)\cos(\phi), \quad k_y = k\sin(\theta)\sin(\phi), \tag{44}$$

where $k = \omega/c$ is the wave number and c is the speed of sound in the incident acoustic medium, θ is the incident angle (measured from z axis) and ϕ is the azimuthal angle. Consequently, the force vector due to the incident pressure field one writes,

$$\mathbf{F}_a = 2\bar{p}_i \int_S \mathbf{N}^T \mathbf{p}_i(\omega) dS. \tag{45}$$

2.5 Vibration and acoustic indicators

The most useful vibration and acoustic indicators used in this work to study the dynamics of composite plate lined with the poroelastic foam are given in the following.

- Mean Square Velocity

The mean square velocity relating the overall behavior of the plate vibration is defined as,

$$v^2 = \frac{1}{2S} \int_S |v|^2 dS, \tag{46}$$

where v is the plate velocity and S is the plate surface.

- Radiated Sound Power

The radiated sound power characterizes the acoustic radiation from the plate and is defined as,

$$\Pi_r = \frac{1}{2} \int_S \text{Re}(pv^*) dS, \tag{47}$$

where p is the radiated sound pressure and v^* is the complex conjugate plate velocity.

- Radiation Efficiency

The non-dimensional radiation efficiency of the plate-acoustic system characterizing the acoustic radiation is defined as the ratio of the acoustic energy radiated by the structure to its potential energy,

$$\sigma = \frac{\Pi_r}{\rho c S v^2}. \tag{48}$$

- Transmission Loss

The transmission loss (TL) on the plate is defined by,

$$\text{TL} = 10\log\left(\frac{\Pi_i}{\Pi_r}\right), \tag{49}$$

where Π_r is the radiated sound power given by Eq. (47) and Π_i is the incident power due to an incident acoustic pressure field. For an incident plane wave excitation the incident power is given by,

$$\Pi_i = \frac{|\tilde{p}_i|^2 \cos(\theta) S}{2\rho_f c_f}, \tag{50}$$

where $\tilde{p}_i$ and θ are the incident pressure field amplitude and the incident angle measured from z axis, respectively, and ρ_f and c_f are the mass density and the speed of sound of the excited acoustic medium, respectively.

- Absorption coefficient

The absorption coefficient of the panel when subjected to an incident acoustic pressure field may be defined as follows,

$$\alpha(\theta, \varphi) = \frac{\Pi_i}{\Pi_d}, \tag{51}$$

where Π_d stands for the dissipated power on the plate.

3 NUMERICAL APPLICATION

In this section a simply supported plate-foam example is considered to assess the proposed numerical approach. Table 1 presents the material properties for an isotropic plate and a poroelastic foam material.

Table 1. Aluminum plate and foam properties.

Plate Al		
Lateral dimensions	0.48×0.42	m^2
Thickness	1	mm
Mass density	2680	kgm^{-3}
Young's modulus	66	GPa
Poisson's ratio	0.33	
Loss factor	0.0	
Foam		
Thickness	3	cm
Porosity	0.98	
Flow resistivity	13500	Nsm^{-4}
Tortuosity	1.70	
Viscous charac. length	20	μm
Thermal charac. length	160	μm
Mass density	30.0	kgm^{-3}
Young's modulus	540	kPa
Poisson's ratio	0.35	
Loss factor	0.01	

The effect fluid loading on the panel vibrations was firstly evaluated considering the plate immersed into two different fluids (air and water) as shown in Fig. 3. In the presence of a heavy fluid the plate response can be significantly modified due to the fluid coupling. On the other hand, the light fluid introduces small variations on the plate vibrations which may justifies the use of simplified acoustic models to compute the vibro-acoustic coupled response of those damped structures immersed in air. In order to firstly validate the presented poroelastic material model, a comparison of real and imaginary parts of the surface impedance of the poroelastic foam layer with the ones of [14] is shown in Fig. 4.
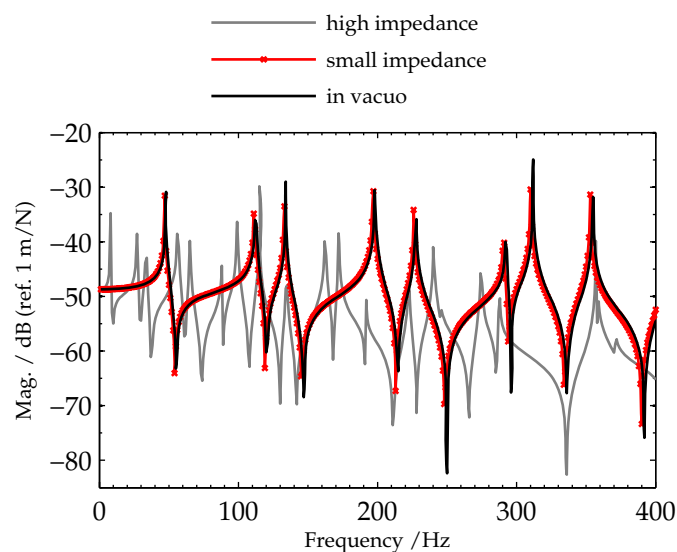
Figure 3. Effect of fluid impedance on the mechanical response of the isotropic plate.
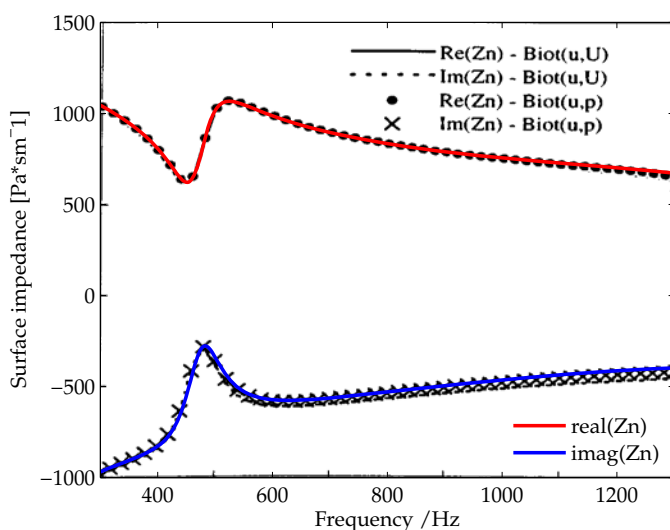

Figure 4. Comparision of surface impedance of laterally infinite poroelastic layer with reference [14].

4 CONCLUSION

In this paper a numerical approach based on the finite element method and Rayleigh integral is developed to simulate vibro-acoustic response of fiber composite materials treated with viscoelastic materials and lined with poroelastic sound absorbing foams. The model allows for taking the fluid loading into consideration by an acoustic impedance matrix. For a plate immersed into a light fluid such air the fluid loading slightly modifies the plate response by a small added mass effect. A partial model validation concerning the poroelastic foam material model is performed.

REFERENCES

[1] R.A.S. Moreira, J. Dias Rodrigues, and A.J.M. Ferreira. A generalized layerwise finite element for multi-layer damping treatments. *Computational Mechanics*, 37(5):426–444, 2006.

[2] M. D. Rao. Recent applications of viscoelastic damping for noise control in automobiles and commercial airplanes. *Journal of Sound and Vibration*, 262(3):457–474, 2003.

[3] R. Moreira and J. D. Rodrigues. Constrained damping layer treatments: Finite element modeling. *Journal of Vibration and Control*, 10(4):575–595, 2004.

[4] R. A. S. Moreira and J. D. Rodrigues. Multilayer damping treatments: Modeling and experimental assessment. *Journal of Sandwich Structures & Materials*, 12(2):181–198, 2010.

[5] O. Foin, J. Nicolas, and N. Atalla. An efficient tool for predicting the structural acoustic and vibration response of sandwich plates in light or heavy fluid. *Applied Acoustics*, 57(3):213–242, 1999.

[6] S. Subramanian, R. Surampudi, K. R. Thomson, and S. Vallurupalli. Optimization of damping treatments for structure borne noise reduction. *Sound and Vibration*, 38(9):14–18, 2004.

[7] S. Assaf, M. Guerich, and P. Cuvelier. Vibration and acoustic response of damped sandwich plates immersed in a light or heavy fluid. *Computers & Structures*, 88(13-14):870–878, 2010.

[8] A. Loredo, A. Plessy, A. El Hafidi, and N. Hamzaoui. Numerical vibroacoustic analysis of plates with constrained-layer damping patches. *Journal of the Acoustical Society of America*, 129(4):1905–1918, 2011.

[9] M. D. Rao, R. Echempati, and S. Nadella. Dynamic analysis and damping of composite structures embedded with viscoelastic layers. *Composites Part B-Engineering*, 28(5-6):547–554, 1997.

[10] S. H. Zhang and H. L. Chen. A study on the damping characteristics of laminated composites with integral viscoelastic layers. *Composite Structures*, 74(1):63–69, 2006.

[11] A. Cummings, H. J. Rice, and R. Wilson. Radiation damping in plates, induced by porous media. *Journal of Sound and Vibration*, 221(1):143–167, 1999.

[12] M. A. Biot. Theory of propagation of elastic waves in a fluid-saturated porous solid .1. low-frequency range. *Journal of the Acoustical Society of America*, 28(2):168–178, 1956.

[13] M. A. Biot. Theory of propagation of elastic waves in a fluid-saturated porous solid .2. higher frequency range. *Journal of the Acoustical Society of America*, 28(2):179–191, 1956.

[14] N. Atalla, R. Panneton, and P. Debergue. A mixed displacement-pressure formulation for poroelastic materials. *Journal of the Acoustical Society of America*, 104(3): 1444–1452, 1998.

[15] N. Atalla, F. Sgard, and C. K. Amedin. On the modeling of sound radiation from poroelastic materials. *Journal of the Acoustical Society of America*, 120(4):1990–1995, 2006.

[16] N. Dauchez, S. Sahraoui, and N. Atalla. Investigation and modelling of damping in a plate with a bonded porous layer. *Journal of Sound and Vibration*, 265(2):437–449, 2003.

[17] P. Goransson. Acoustic and vibrational damping in porous solids. *Philosophical Transactions of the Royal Society A*, 364(1838):89–108, 2006.

[18] O. Doutres, N. Dauchez, and J. M. Genevaux. Porous layer impedance applied to a moving wall: Application to the radiation of a covered piston. *Journal of the Acoustical Society of America*, 121(1):206–213, 2007.

[19] P. Debergue, R. Panneton, and N. Atalla. Boundary conditions for the weak formulation of the mixed (u,p) poroelasticity problem. *Journal of the Acoustical Society of America*, 106(5):2383–2390, 1999.

[20] F. Fahy and P. Gardonio. *Sound and structural vibration: radiation, transmission and response*. Elsevier, London, 2nd edition, 2007.

[21] N. Atalla and J. Nicolas. A new tool for predicting rapidly and rigorously the radiation efficiency of plate-like structures. *Journal of the Acoustical Society of America*, 95(6): 3369–3378, 1994.

[22] J. F. Allard and Noureddine Atalla. *Propagation of sound in porous media: modelling sound absorbing materials*. Wiley-Blackwell, Oxford, 2nd edition, 2009.